Experimental and theoretical studies of (E)−N′−1−(4−propylbenzylidene)nicotinohydrazide as corrosion inhibitor of mild steel in 1 M HCl

ARTICLE *in* PROTECTION OF METALS AND PHYSICAL CHEMISTRY OF SURFACES · MAY 2015

Impact Factor: 0.74 · DOI: 10.1134/S2070205115030041

6 AUTHORS, INCLUDING:

Paul A L Anawe

Covenant University Ota Ogun State, Nigeria

8 PUBLICATIONS **1** CITATION

SEE PROFILE

Ogunniran Kehinde Olurotimi

Covenant University Ota Ogun State, Nigeria

24 PUBLICATIONS **97** CITATIONS

SEE PROFILE

Cyril Ehi-Eromosele

Covenant University Ota Ogun State, Nigeria

26 PUBLICATIONS **8** CITATIONS

SEE PROFILE

ISSN 2070-2051, Protection of Metals and Physical Chemistry of Surfaces, 2015, Vol. 51, No. 3, pp. 458–466. © Pleiades Publishing, Ltd., 2015.

PHYSICOCHEMICAL PROBLEMS OF MATERIALS PROTECTION

Experimental and Theoretical Studies of (*E*)-*N*'-1-(4- propylbenzylidene)nicotinohydrazide as Corrosion Inhibitor of Mild Steel in 1 M HCl[1]

P. A. L. Anawe[a], C. U. Obi[a], S. S. Mehdi[b], K. O. Ogunniran[c], B. I. Ita[c], and C. O. Ehi-Eromosele[c]

[a] *Department of Petroleum Engineering, Covenant University, PMB 1023, Ota, Nigeria*
[b] *Department of Chemistry, College of Science, Al-Nahrain University, Baghdad-Iraq*
[c] *Department of Chemistry, Covenant University, PMB 1023, Ota, Nigeria*
e-mail: cyril.ehi-eromosele@covenantuniversity.edu.ng

Received July 22, 2014

Abstract—The efficiency of a novel Schiff base namely (*E*)-*N*'-1-(4-propylbenzylidene)nicotinohydrazide (PBNH) was investigated as corrosion inhibitor of mild steel (MS) in 1M HCl using weight loss technique at 303 and 313 K. It was established that corrosion rate of mild steel increases with increase in temperature and concentration of HCl. Results showed that PBNH considerably inhibited the corrosion of mild steel in a 1 M HCl solution and inhibition efficiency is about 70% at 4×10^{-4} M PBNH at both temperatures. The inhibition efficiency of PBNH increased with an increase in concentration and temperature. The adsorption model obeys the Langmuir adsorption isotherm and the kinetic–thermodynamic model and the value of free energy of adsorption, ΔG_{ads} indicated that the adsorption of PBNH was a spontaneous process and was both an electrostatic-adsorption (physisorption) and adsorption on the basis of donor-acceptor interactions (chemisorption). Thermodynamic parameters calculated show the spontaneity and endothermic nature of the process and also reveal the favourable affinity of PBNH towards the mild steel surface. Quantum chemical calculations based on PM3 method was performed on PBNH and calculated parameters gave useful information to explain the interaction between the surface of metal and PBNH.

DOI: 10.1134/S2070205115030041

1. INTRODUCTION

Corrosion remains a big problem to general processes involving metals. For example, in the Nigeria's oil and gas industry, corrosion accounts substantially for oil pipeline failures [1]; this has led to environmental pollution, accidents and adverse effect on the economy in terms of the cost of corrosion control methods.

The most common form of corrosion occurs when steel comes in contact with an aqueous environment and rusts. The corrosion of iron or mild steel in acidic media has been studied extensively, especially for its industrial relevance [2]. In fact, acid solutions widely used in cleaning, descaling, pickling, and oil well acidizing, require the use of corrosion inhibitors to reduce their corrosion attack on metallic structures or materials [2–5]. Among the methods of monitoring corrosion rate, the weight loss method is still very useful because of its simple application and reliability [6, 7].

The use of organic compounds as corrosion inhibitors may be the main choice to decrease the corrosion rate of alloys in acidic media [8]. Numerous studies have been done on corrosion inhibition of steel by organic compounds in acidic medium and they have proved to be effective and efficient [8–13]. The corrosion inhibition property of these compounds is attributed to their molecular structure. The planarity and lone pair electrons present in hetero-atoms determine both the efficiency and adsorption mechanism [8, 9, 14, 15].

Hydrazine, an inorganic compound, is known to be used as an oxygen scavenger and corrosion inhibitor in boiler water treatment. However due to the toxicity and certain undesired effects this practice is discouraged. The present work is undertaken to synthesize a hydrazine derivative, (*E*)-*N*'-1-(4-propylbenzylidene) nicotine-hydrazide, characterise the as-synthesised compound, and evaluate the inhibition efficiency of this as-synthesized compound in controlling corrosion of mild steel in HCl solution by weight loss method. The adsorption behavior was studied to determine the adsorption isotherm and thermodynamic data. Theoretical studies on electronic and molecular structures of PBNH were conducted using quantum chemical calculations.

[1] The article is published in the original.

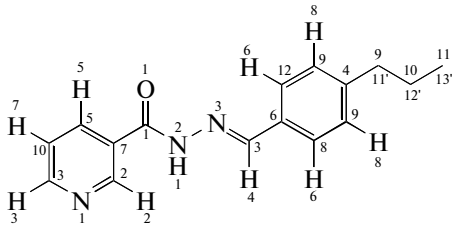

Fig. 1. The PBNH structure.

2. EXPERIMENTAL

2.1. Mild Steel Specimen

Corrosion inhibition tests were performed using specimens prepared from a sheet of mild steel (MS), having the composition C = 0.12%, Mn = 0.90%, S = 0.066%, P = 0.050%, Si = 0.10% and remainder Fe. The sheet with a thickness of 2 mm was mechanically press-cut into 5 × 4 cm coupons and holes of about 0.02 cm in diameter were drilled on the centre of the shorter sides of all the coupons for the insertion of glass hooks for suspension. The total geometric surface area was approximately 40.0 cm^2 and the average weight of a coupon was 33 g. The coupons were polished with 600 grade emery paper, degreased in absolute ethanol and cleaned by mild scrubbing with bristle brush, rinsed in absolute ethanol again and then dried in acetone. These coupons were then stored in a desiccator in the absence of moisture before their use for the investigation. Each specimen of MS was weighted immediately before the suspension in the cell.

2.2. Preparation of the PBNH

PBNH has the structure reported in Fig. 1.

The synthetic methods described by Abeda Jamadar et al. [16] were modified and adopted for the synthesis of acylhydrazones in this work. The nicotinic acid hydrazide (10 mmol, 171 mg) was dissolved in absolute ethanol (20 mL) by heating gently on water bath after which the 4-propylbenzaldehyde in absolute ethanol (10 mmol, 148 mg) was added. Two drops of acetic acid was added and refluxed for 48 h (Fig. 2). The precipitate obtained was allowed to stay at ambient temperature for 12 h, after which it was recrystallized in the mixture of chloroform and methanol (2 : 8). The product obtained was filtered, washed thrice with 30 mL of absolute methanol and was dried in the vacuum. The purity of the compound was confirmed by TLC (10% methanol : 90% chloroform).

2.3. Preparation of Solutions

Solution of 1 M HCl was prepared from commercial analytical reagent using distilled water from which increasing concentrations were prepared. The PBNH used as inhibitor was prepared in concentrations of 0.0001 to 0.0005 M in the increment of 0.0001 in 1 M HCl solution. The prepared additive solutions were used for all measurements.

2.4. Weight Loss Measurements

The weight loss (WL) measurements were carried out using the procedures outlined in Ita [17]. Five 250 mL beakers which separately contained 1, 1.5, 2, 2.5, and 3 M HCl solutions, were placed in three thermostat baths maintained at 30, 40 and 50°C, constituting three sets of experiments. The weighed coupons were each suspended in a beaker with the help of glass hooks and glass rods. These coupons were retrieved at 1 h intervals progressively for 7 h. Each retrieved coupon was washed several times in 20% NaOH containing 200 g/L of zinc dust until clean, dried in acetone and reweighed. The weight was evaluated in grams. A reading reported represented the average of three readings recorded on a Mettler H 35 AR analytical

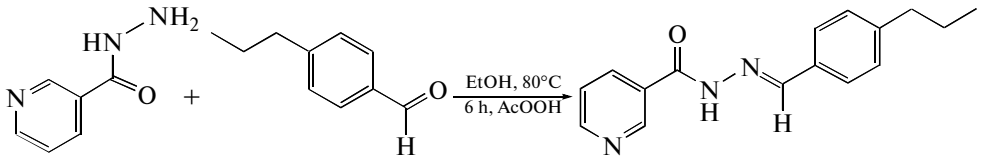

Fig. 2. The synthesis of PBNH.

The structure of the compound was characterized by ^{1}H NMR, ^{13}C NMR, MS and FTIR spectroscopic methods.

yield 2.32g (86.89%); **mp**: 107–109°C; R_f = 0.82 ($CHCl_3$/CH_3OH, 4 : 1, at RT).

^{1}H-NMR (DMSO-d_6) δ: 11.92 (s, 1H, NH), 9.02 (s, 1H, H(2)), 8.72 (d, J = 4.29 Hz, 1H, H(3)), 8.37 (s, 1H, H–C=N), 8.22 (d, J = 7.53 Hz, 1H, H–C(5)), 7.62 (dd, J = 7.50 Hz, 2H, H(6)), 7.53 (t, 1H, J_1 = 5.61 Hz, J_2 = 6.53 Hz, H(7)), 7.24 (dd, J = 7.50 Hz, 2H, H(8)), 2.56 (t, J = 7.23 Hz, 2H of CH_2, H(9)), 1.58 (m, J_1 = 7.26 Hz, J_2 = 6.93 Hz, 2H of CH_2, H(10)), 0.867 (t, J = 7.17 Hz, 3H of CH_3, H(11)) ppm.

^{13}C-NMR (DMSO-d_6) δ: 162.09 (CO), 152.03 (C(2)), 149.03 (2C(3)), 145.02 (C(4)), 135.89 (C(5)), 132.17 (C(6)), 129.70 (C(7)), 129.32 (2C(8)), 127.67 (2C(9)), 124.06 (C(10)), 37.59 (C(11)), 24.31 (C(12)), 14.06 (C(13)) ppm.

IR (KBr) cm^{-1}: 3445 (enol OH), 3216 (NH), 1651 (C=O), 1600 (C=N), 1418 (N–N), 1292 (C–O), 1147 (C–N).

MS (ESI+): in m/z: 258.1 $[M + H]^+$.

Anal. calcd. for $C_{16}H_{17}N_3O$ (267.14): C, 71.89; H, 6.41; N, 15.72. Found: C, 71.51; H, 6.23; N, 17.39.

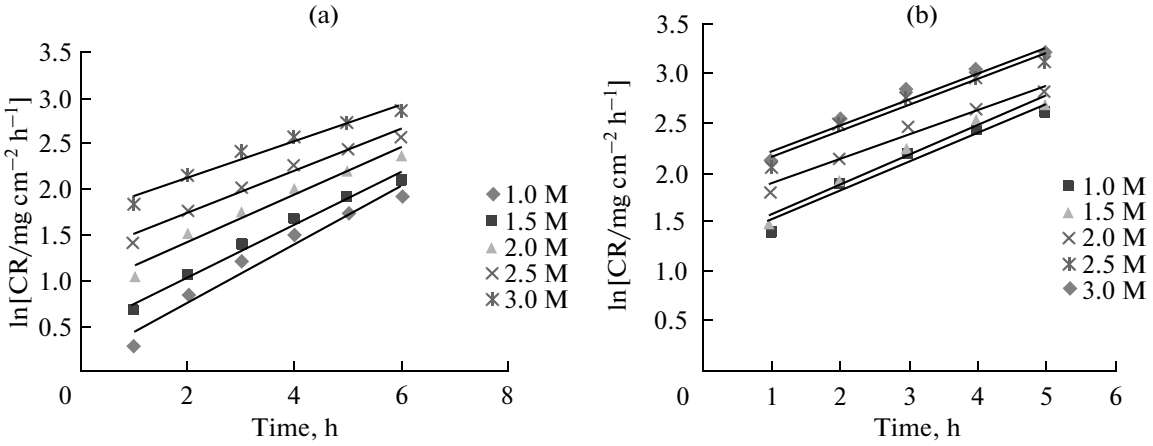

Fig. 3. Variation of logarithm of corrosion rate with time for mild steel in different concentrations of HCl solutions at (a) 30°C, (b) 40°C.

balance to the nearest 0.0001 g. Further measurements using weight loss determination involved the introduction of the inhibitors into three sets each of five beakers maintained at 30, 40, 50°C. Each previously weighed mild steel coupon was introduced into the beakers containing PBNH. The experiments in the presence of the additives were performed differently. As described earlier, each coupon was also retrieved from the corrodent HCl–inhibitor solutions every 1 h for the period of 7 h, washed and weighed. The difference in weight of the coupons was taken as the weight loss (*WL*) defined as:

$$WL = W_o - W_t, \quad (1)$$

were W_o and W_t (mg) are the initial and final weights respectively of the specimen after a 1 h immersion in acidic solution without or with inhibitor.

Weight loss allowed calculation of the mean corrosion rate (*CR*) in (mg cm^{-2} h^{-1}). The corrosion rate of mild steel was determined using the relation:

$$CR = \frac{WL}{At}, \quad (2)$$

where *A* is the area and *t* is the immersion period.

The percentage inhibition efficiency (*IE* (%)) was calculated using the relationship [1]:

$$IE = \frac{\Delta W_o - \Delta W_t}{\Delta W_o} \times 100 = \theta_{WL} \times 100, \quad (3)$$

where θ is the degree of surface coverage.

2.5. Computational Studies

In order to gain insight into the electronic configuration and inhibitive capability of PBNH, quantum chemical calculations were performed using the semi-empirical calculations with PM3 method [18]. The Hyperchem Program with complete geometry optimization was used. The molecular orbitals, E_{HOMO} (the energy of the highest occupied molecular orbital) and E_{LUMO} (the energy of the lowest unoccupied molecular orbital) were analyzed and this helps to find out from molecular structure of PBNH the possible sites of nucleophilic and electrophilic reactions with the mild steel surface. The optimized molecular structures are shown in Fig. 5 and the calculated energies E_{HOMO}, E_{LUMO}, energy gap ($E = E_{HOMO} - E_{LUMO}$) and other indices are given in Table 4.

Table 1. Weight losses (*WL*), corrosion rates (*CR*), surface coverage (θ) and inhibitor efficiency [*IE* (%)] obtained in weight loss tests after 5 h of MS specimens immersion time in 1 M HCl (blank solution) or in PBNH solutions at 303 K and 313 K

C (M)	*WL* (g)		*CR* (mg cm^{-2} h^{-1})		θ		*IE* (%)	
	303 K	313 K	303 K	313 K	303 K	313 K	303 K	313 K
Blank	0.2266	0.5403	1.13	2.70	–	–	–	–
0.0001	0.2223	0.2573	1.11	1.29	0.019	0.524	1.90	52.40
0.0002	0.2094	0.2197	1.05	1.10	0.076	0.593	7.59	59.34
0.0003	0.1098	0.1921	0.55	0.96	0.515	0.644	51.54	64.45
0.0004	0.0693	0.1722	0.35	0.86	0.694	0.681	68.13	69.42

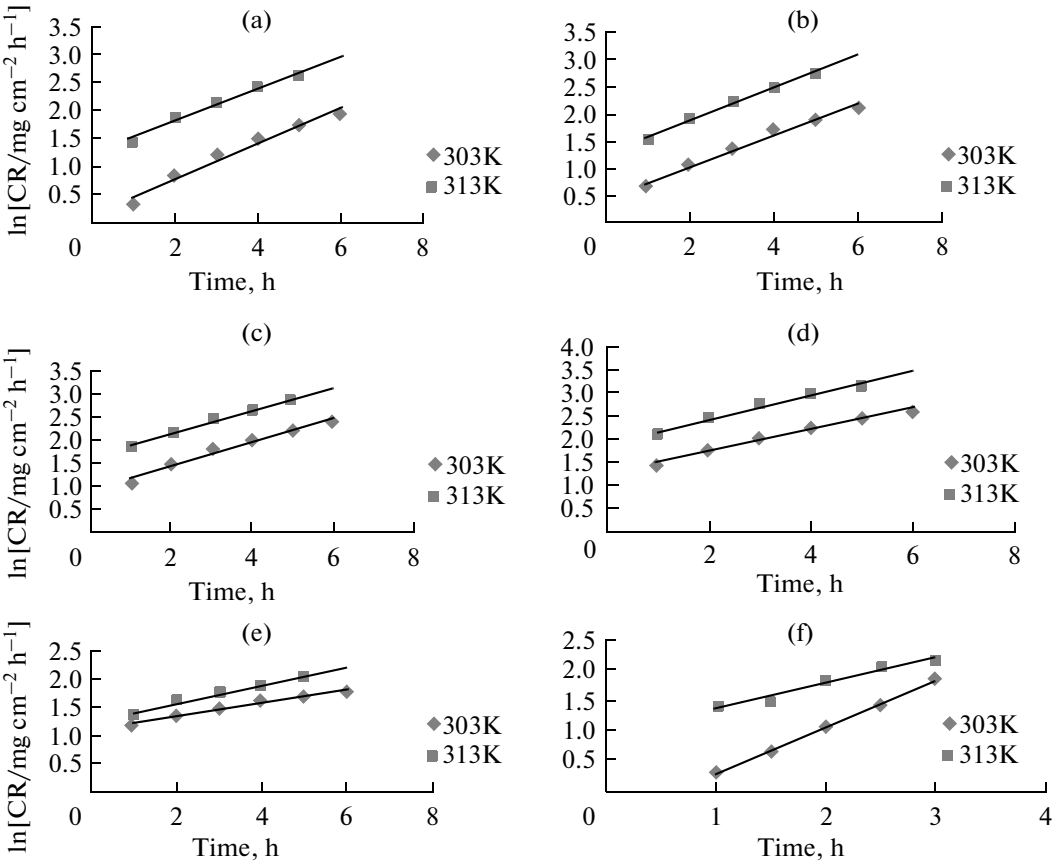

Fig. 4. Dependence of temperature variation on the corrosion rate with time for mild steel in HCl (a) 1 M, (b) 1.5 M, (c) 2 M, (d) 2.5 M, (e) 3 M at 303K and 313K and (f) variation of logarithm of corrosion rate with HCl concentration.

3. RESULTS AND DISCUSSION

3.1. Effect of Corrodent Concentration on Corrosion Rate of Mild Steel in HCl Solution

The corrosion rate of mild steel in hydrochloric acid solution at different concentrations was studied by weight loss at two temperatures, 30°C (303 K) and 40°C (313 K) at one hour of immersion period. The variation of the logarithm of the corrosion rate of mild steel in increasing concentrations of HCl with time is shown in Fig. 3.

The results indicate that the corrosion rate of mild steel increases with increase in concentration of HCl acid and with time (increasing hours of exposure of the mild steel to acid). Similar results have been reported elsewhere [19]. This could be attributed to increased concentration of the chloride ions in the more concentrated solution, which readily react with the iron ions present in the solutions [19] and also the increased solubility of the iron chloride product.

3.2. The Dependence of Temperature on Corrosion Rate of Mild Steel in HCl Solution

The dependence of temperature variation on the corrosion rate with time for mild steel in HCl is shown in Fig. 4a–4e. All the plots show an increase in corrosion rate as the temperature increased from 303 K to 313 K. It is a well known fact that temperature increases the rate of all electrochemical processes and influences adsorption equilibrium and kinetics as well. Figure 4f shows a linear relationship between the logarithm of the corrosion rate and concentration of HCl which indicates the absence of insoluble product on the mild steel surface [20]. An increase in the corrosion rate of mild steel as temperature increased is also observed at a given concentration of acid (Fig. 4f).

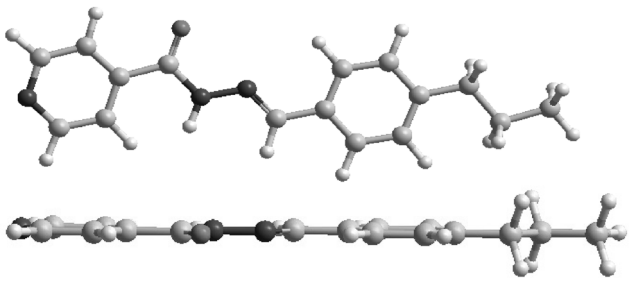

Fig. 5. More energetically stable conformations of PBNH with PM3 method.

Table 2. The Adsorption parameters from Langmuir isotherm, Freundlich isotherm and kinetic–thermodynamic models for the adsorption of PBNH in 1M HCl on the mild steel after 7 h of immersion time at 303 K and 313 K

	Langmuir isotherm model			
T (K)	K_{ads} (M^{-1})	ΔG°_{ads}, kJ/mol		R^2
303	167	−23.01		0.876
313	14.286	−35.35		0.998
	Freundlich isotherm model			
T (K)	K_{ads} (M^{-1})	n	ΔG°_{ads}, kJ/mol	R^2
303	1.4×10^9	2.735	−63.17	0.972
313	2.83	0.183	−13.16	0.997
	Kinetic-thermodynamic model			
T (K)	K_{ads} (M^{-1})	y	ΔG°_{ads}, kJ/mol	R^2
303	3.040	6.440	−30.32	0.982
313	11.583	0.473	−34.80	0.988

3.3. Effect of Inhibitor Concentration

A series of weight loss measurements were carried out after 7 h immersion in 1.0 M HCl in the absence and presence of various concentrations of the inhibitor (PBNH). Table 1 shows the calculated values of weight loss, surface coverage, corrosion rate and inhibition efficiencies at 303 K and 313 K. The results show that the corrosion inhibition efficiencies and surface coverage of PBNH increase with increasing inhibitor concentration. The corrosion rate decreased considerably with an increase in concentration of inhibitor. The increase in efficiency of inhibition with concentration of inhibitors indicates that more inhibitor molecules are adsorbed on the metal surface at higher concentration, leading to greater surface coverage. These results are similar to the ones reported by [7, 9].

3.4. Effect of Temperature

The results from Table 1 show that the investigated PBNH had inhibiting properties at both temperatures and the inhibition efficiency of PBNH increase with increase in temperature. Thus, the studied inhibitor efficiency is temperature dependent [7]. The general increase in inhibition efficiency observed with increased temperature for PBNH is suggestive of the existence of very strong adsorption interaction between the mild steel surface and the inhibitors which is chemical in nature [17, 21]. It can also be seen that the corrosion rate at the same inhibitor concentration increase with increase in temperature, a trend that is similar to corrosion rate in the absence of inhibitors (Fig. 4a), but was lesser than the corrosion rate without inhibitor clearly showing an inhibition of corrosion of mild steel in HCl.

3.5. Adsorption Mechanism of PBNH

The adsorption of organic molecules at the metal/solution interface consists of the replacement of water molecules by organic molecules according to following process [22]:

$$Org_{(sol)} + yH_2O_{(ads)} \rightleftharpoons Org_{(ads)} + yH_2O_{(sol)},$$

where $Org_{(sol)}$ and $Org_{(ads)}$ are organic molecules in the solution and adsorbed on the metal surface, respectively, and y is the number of water molecules replaced by the organic molecules. The adsorption of this organic compound and by extension its inhibitory efficiency is influenced by electronic structure, steric factor, electronic density at donor site, presence of functional groups, molecular area and molecular weight [2, 23–25].

The values in Table 1 clearly indicate that mild steel corrosion is reduced by the presence of PBNH inhibitor in 1M HCl at all the concentrations and temperatures used in this study. This can be explained by the adsorption of PBNH on the mild steel surface. The efficiency of an organic compound as an inhibitor is mainly dependent on its ability to get adsorbed on metal surface [2]. This interaction between the metal surface and the inhibitor can be explained by the adsorption isotherms. An equation that relates the

Table 3. Thermodynamic parameters for the inhibition of MS in 1 M HCl solution containing PBNH from weight loss measurements

Concentration of inhibitor, M	Activation energy, E_a, (kJ/mol)	ΔG°_{ads}, kJ/mol		ΔH°_{ads}, kJ/mol	ΔS°_{ads} J mol^{-1} K^{-1}	
		303 K	313 K		303 K	313 K
		−30.32	−31.80	106	450	
0.0001	0.012					
0.0002	0.004					
0.0003	0.044					
0.0004	0.071					

Table 4. Calculated quantum chemical parameters of PBNH using PM3 method

Inhibitor	HOMO (eV)	LUMO (eV)	$\Delta E(E_{HOMO} - E_{LUMO})$ (eV)	μ (Debye)	Planarity
PBNH	−8.80862	−0.88299	−7.92563	3.45	Semiplanar

amount of substance attached to a surface to its concentration in gas phase or in solution at fixed temperature is known as an adsorption isotherm. The simplest one is the Langmuir isotherm which is represented as:

$$\frac{c}{\theta} = \frac{1}{k_{ads}} + C \quad (4)$$

where C is the inhibitor concentration, K_{ads} is the adsorption equilibrium constant and θ is the surface coverage. Systems that obey this equation are often referred to as ideal adsorption.

Nonideal system can sometimes be fitted to an empirical adsorption isotherm of Freundlich:

$$\log\theta = \log K_{ads} + n\log C, \quad (5)$$

where $0 < n < 1$. K_{ads}, is adsorptive equilibrium constant, C is inhibitor concentration, n is related to the adsorption intensity, and (θ) is surface coverage.

Recent researches have looked into the action of adsorptive inhibitors from purely mechanistic kinetic point of view [26, 27]. A kinetic–thermodynamic model for adsorption process at metal-solution interface has been suggested. This model has been tested on inhibition effect of number of open chain amines and on macrocyclic amine on the corrosion of steel in H_2SO_4 [28] and Copper–Nickel Alloy in HCl [27]. In this model, (y) is the number of inhibitor molecules occupying one active site. This model can be given by the following equation:

$$\log\left[\frac{\theta}{(1-\theta)}\right] = \log K' + y\log C, \quad (6)$$

y is the number of inhibitor molecules occupying one active site (or the number of water molecules replaced by one molecule of PBNH). K' is a constant which is related to the adsorptive equilibrium constant by [27]:

$$K_{ads} = (K)'^{1/y}. \quad (7)$$

Afterward, the standard free energy of inhibitor adsorption, ΔG°_{ads}, on metal surface can be calculated using the following equation:

$$\Delta G^{\circ}_{ads} = -RT\ln(55.5K_{ads}). \quad (5)$$

In this expression, R is gas constant, T is absolute temperature and 55.5 is molar concentration of water in one liter solution.

Therefore, the surface coverage θ values for the PBNH obtained from weight loss measurements reported in table 1 were analysed in order to determine the type of adsorption isotherm they fit into, which provides evidence about the inhibition mechanism.

The higher value of K_{ads} indicates that the inhibitor is strongly adsorbed on the metal surface [27] and that the adsorption process is more favourable than the desorption process [22]. Earlier, it has been established that for the same concentration of PBNH inhibitor used, the inhibition efficiency increases with an increase in temperature, indicating an endothermic process (see Table 1). This might be attributed to the increased surface coverage at higher temperatures, expansion and creation of active and reactive sites. From the values of K_{ads} in Table 2, only the Langmuir isotherm and kinetic–thermodynamic model can account for the increase in inhibition efficiency with increase in temperature. In both cases, linear plots were obtained, which reveal the applicability of these isotherms on the ongoing adsorption process. Ideally, the adsorption isotherms should have gradients equal to 1. The deviation from unity might be due to the interaction among the adsorbed species on the metal surface mostly when using organic molecules. Although the Freundlich isotherm had comparable good correlation coefficients, its values of K are suggestive of a decrease of inhibition efficiency with increase in temperature. Moreover, the value of n at 303 K is greater than 1 which disagrees with typical values of $0 < n < 1$.

Generally, values of ΔG°_{ads} up to −20 kJ/mol are consistent with the electrostatic interaction between the charged molecules and the charged metal (physisorption), while those between −40 and −400 kJ/mol are associated with chemisorption as a result of sharing or transferring of electrons from the inhibitor molecules to the metal surface to form a coordinated type of bond [2, 29]. PBNH possesses unshared pairs of electrons on the nitrogen and oxygen atoms, which can interact with d-orbitals of MS surface to give the adsorbed protective film. The calculated ΔG°_{ads} values (around −23 to −35 kJ/mol), lower than −20 kJ/mol but not as low as −40 kJ/mol and more, indicated that the PBNH adsorption mechanism on MS surface in 1 M HCl solution after 7 h was more than an electrostatic-adsorption, but not a true chemisorption [2, 22]. Temperature increase is known to accelerate chemisorption of the inhibitor on the metal surface. If in a series of experiments the temperature increase causes an inhibition efficiency increase, especially when the ΔG°_{ads} diminishes reaching values lower than −40 kJ/mol, the inhibitor adsorption is recognized as

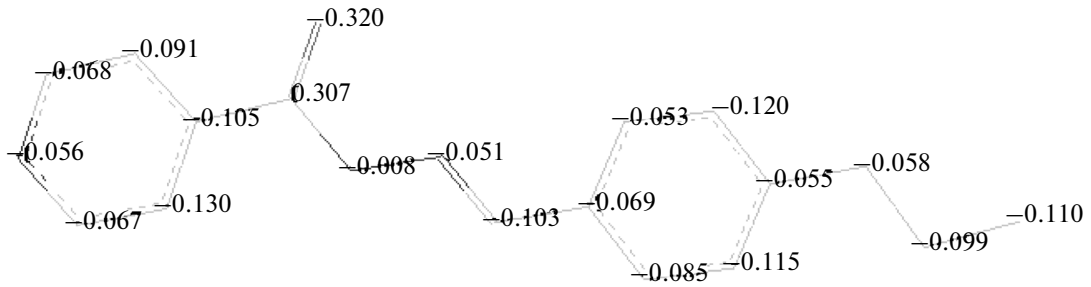

Fig. 6. The charge density distribution of the PBNH molecule.

a chemisorption, involving an out-and-out sharing or transfer of electrons [2, 30, 31]. In this experiment, temperature increase resulted in increased inhibition efficiency for PBNH but ΔG°_{ads} values were not lower than −40 kJ/mol and not higher than −20 kJ/mol. This further supports the conclusion that PBNH adsorption mechanism ranges between a physisorption and chemisorption.

3.6. Thermodynamic Treatment of Weight Loss Result with Inhibitor

The thermodynamic parameters were calculated from the kinetic-thermodynamic model to further elucidate the ongoing process. The following equations were used:

$$\Delta H^{\circ}_{ads} = R\frac{T_1 T_2}{T_2 - T_1}\ln\frac{K_2}{K_1}, \quad (6)$$

$$\Delta S^{\circ}_{ads} = \frac{\Delta H^{\circ}_{ads} - \Delta G^{\circ}_{ads}}{T}, \quad (7)$$

where K_1 and K_2 are the equilibrium adsorption constants at 303 and 313 K respectively and obtained from the slopes of the kinetic-thermodynamic adsorption isotherms.

The activation energy values obtained in the study were computed from the transformed.

Arrhenius equation:

$$E_a = \left(2.303R\frac{T_1 T_2}{T_2 - T_1}\right)\left(\log\frac{\rho_2}{\rho_1}\right), \quad (8)$$

where R is the molar gas constant, ρ_1 and ρ_2 are corrosion rates at T_1 and T_2 respectively [32].

The calculated thermodynamic parameters, activation energy (E_a), change in standard free energy of adsorption (ΔG°_{ads}), change in enthalpy of adsorption (ΔH°_{ads}), change in entropy of adsorption (ΔS°_{ads}) are presented in Table 3. The activation energy generally increased with an increase in the concentration of the inhibitor which justifies the conclusion that inhibition efficiency increases with increase in inhibitor concentration. The low values of the activation energies of the inhibitor obtained are suggestive of physical adsorption. The negative values of ΔG°_{ads} establishes the feasibility of the adsorption process. In addition, the decrease in values of ΔG°_{ads} with increasing temperature shows the spontaneity of the process at higher temperatures. It is interesting that the ΔH°_{ads} value is positive further confirming the endothermic nature of the process and the positive value of ΔS°_{ads} reveals the favourable affinity of the inhibitor towards the metal surface.

These results show that adsorption is not always an exothermic process ($\Delta H^{\circ}_{ads} < 0$) as some literatures report. Adsorption processes can be either exothermic or endothermic. In exothermic process, adsorption normally decreases with an increase in temperature while in endothermic process the adsorption increases with increase in temperature. This happens sometimes in adsorption processes in the liquid phase like the one used in this experiment (PBNH solution/mild steel).

3.7. Theoretical Studies

Quantum chemical calculations have been proved to be a very powerful tool for studying the mechanism of corrosion inhibition [33]. To study the relationship between molecular structure and inhibitive effect of PBNH, we used molecular orbitals of semi-empirical calculations with PM3 method. PBNH, on molecular structural considerations, has adsorption centers that is, N (C=N) and O (C=O). All the theoretical quantum calculations of PBNH were performed using more energetically stable conformations in gas phase at 25°C (Fig. 5). Table 4 shows the calculated quantum chemical parameters like E_{HOMO}, E_{LUMO} and μ (dipole moment) of PBNH inhibitor.

The frontier molecule orbital density distributions for PBNH are shown in Fig. 7. Frontier orbital theory is useful in predicting adsorption centers of the inhibitor molecules responsible for the interaction with surface metal atoms [34, 35]. Depending on the presence

of N and O atoms in PBNH inhibitor, the repartition density of the HOMO and LUMO is preferentially localized on N (C=N) and O (C=O) atoms for PBNH molecule. EHOMO measures the tendency of donating electron by a molecule while ELUMO indicates the ability of the molecule to accept electrons [36]. The interaction between the inhibitor and the metal is through the donation of the electrons from the inhibitor occupied orbitals (mainly from the HOMO) to the *d* orbital of the metal [33], and also through the acceptance of the electrons from the *d* orbital of the metal to the unoccupied orbitals (mainly to the LUMO) of the inhibitor. Good inhibitors are those which not only offer electrons to the unoccupied d orbital of the metal atom, but have good tendency to accept and accommodate electrons in their unoccupied orbitals [37]. Quantum chemical parameters listed in Table 4 reveal that PBNH has high HOMO and low LUMO with high energy gap. The number of transferred electrons (ΔN) was also calculated according to Eq. (9) [38, 39].

$$\Delta N = (X_{Fe} - X_{inh})/[2(\eta_{Fe} - \eta_{inh})], \quad (9)$$

where X_{Fe} and X_{inh} denote the absolute electronegativity of iron and the inhibitor molecule, respectively; η_{Fe} and η_{inh} denote the absolute hardness of iron and the inhibitor molecule, respectively. The theoretical values of X_{Fe} and η_{Fe} are 7 and 0 eV/mol, respectively [38]. These quantities are related to electron affinity (A) and ionization potential (I).

$$X = (I + A)/2, \quad (10)$$

$$\eta = (I - A)/2. \quad (11)$$

The softness, σ is the inverse of the hardness [40],

$$\sigma = 1/\eta. \quad (12)$$

I and A are related in turn to E_{HOMO} and E_{LUMO}

$$I = -E_{HOMO}, \quad (13)$$

$$A = -E_{LUMO}. \quad (14)$$

Values of X and η were calculated by using the values of I and A obtained from quantum chemical calculation.

Other calculated quantum chemical parameters are reported in Table 5.

Electronegativity, hardness, and softness have proved to be very useful quantities in chemical reactivity theory. When two systems, Fe and inhibitor, are brought together, electrons will flow from lower X_{inh} to higher X_{Fe}, until the chemical potentials become equal [36]. The value of ΔN showed inhibition effect resulted from electrons donation [33, 38, 39]. If $\Delta N < 3.6$, the inhibition efficiency increases by increasing the electron-donating ability of these inhibitors to donate electrons to the metal surface [39]. In this study, PBNH was the donor of electrons while mild steel surface was the acceptor. The PBNH was bound to the mild steel surface, and thus formed inhibition adsorption layer against corrosion.

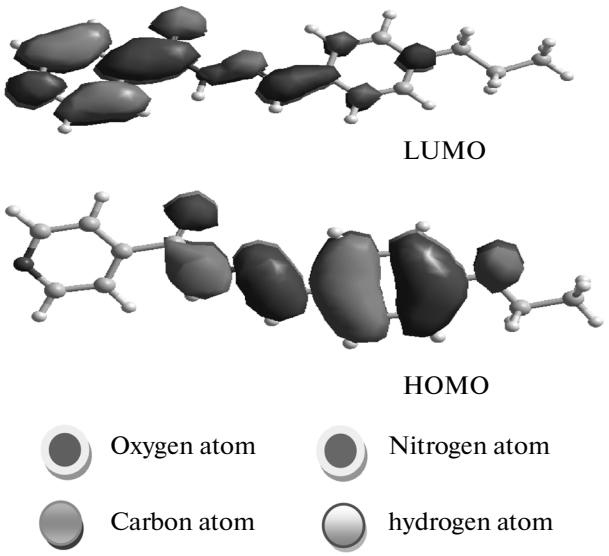

Fig. 7. The frontier molecular orbital density distributions (HOMO and LUMO) using PM3 Method.

The charge density distribution of the PBNH molecule is given in Fig. 6. It can be seen that oxygen, nitrogen and some carbon atoms have higher charge densities. Generally, the electrophiles attack the regions of highest electron density. Therefore, oxygen, nitrogen and carbon atoms were the active centers, which had the strongest ability of bonding to the ferrous surface. In addition, it can be seen that HOMO (Fig. 7) was mainly distributed on the area containing oxygen atom. Thus, the area containing oxygen atom was probably the primary site of the bonding.

From the chemical quantum calculations, it could be deduced that PBNH molecules can be directly adsorbed at the mild steel surface on the basis of donor-acceptor interactions (electrostatic attraction) and can also be adsorbed on the mild steel surface using a number of active centers that can form protective layer on the mild steel surface, thus inhibiting the corrosion of the metal.

4. CONCLUSIONS

The use of (*E*)-*N*'-(1-(4-propylbenzylidene)nicotinohydrazide) (PBNH) as a corrosion inhibitor of

Table 5. Calculated quantum chemical parameters of PBNH molecule

Inhibitor	I (au)	A (au)	X (au)	η (au)	σ (au^{-1})	ΔN
PBNH	8.80862	0.88299	4.84581	3.96282	0.25235	–0.27189

mild steel (MS) was assessed in 1 M HCl at 303–313 K temperature range after 7 h immersion time using WL measurements. Quantum chemical calculations were also used to study the correlation of the electronic and molecular structures of PBNH with its inhibitive properties. The conclusions of this work can be summarized as follows:

1. Corrosion rate of mild steel increases with increase in temperature and concentration of HCl.

2. MS corrosion is reduced by the presence of PBNH inhibitor in 1 M HCl at all the concentrations and temperatures used in this study. The inhibition efficiency of PBNH increased with an increase in concentration and temperature indicating an endothermic process.

3. The adsorption model obeys the Langmuir adsorption isotherm and the kinetic-thermodynamic model. The obtained value of ΔG°_{ads} indicates that the adsorption of PBNH molecule was a spontaneous process and PBNH adsorption mechanism on mild steel surface was both an physisorption and chemisorptions.

4. The activation energy generally increased with an increase in the concentration of the inhibitor confirming the conclusion that inhibition efficiency increased with increase in inhibitor concentration. Positive ΔH°_{ads} value is further confirms the endothermic nature of the process and the positive value of ΔS°_{ads} reveals the favourable affinity of the inhibitor towards the metal surface.

5. Quantum chemical calculations also show that the interaction of PBNH molecule with the mild steel surface is through electrostatic attraction (physisorption) and through adsorption using oxygen, nitrogen and carbon atoms as its active centers (chemisorption). The area containing O atom is most probable site for bonding the mild steel surface by donating electrons to the metal.

6. The inhibitor used has a melting point of 107–109°C compared to that of hydrazine which is 2°C. Previously used as an antituberculant, this inhibitor is far less toxic compared to hydrazine.

REFERENCES

1. Achebe, C.H., Nneke, U.C., and Anisiji, O.E., *Proceedings International MultiConference of Engineers and Computer Scientists,* 2012, vol. 2, p. 1.
2. Moretti, G., Guidi, F., and Fabris, F., *Corros. Sci.,* 2013, vol. 76, p. 212.
3. Lagrenée, M., Mernari, B., Bouanis, M., et al., *Corros. Sci.*, 2002, vol. 44, p. 573.
4. Bommersbach, P., Alemany-Dumont, C., Millet, J.P., et al., *Electrochim. Acta*, 2005, vol. 51, p. 1076.
5. Pierre, F., Moinet, C., and Toupet, L., *J. Organomet. Chem.*, 1997, vol. 527, p. 60.
6. Obot, I.B., Obi-Egbedi, N.O., and Umoren, S.A., *Corros. Sci.*, 2009, vol. 51, p. 1868.
7. Behpour, M., Ghoreishi, S., Mohammadi, N., et al., *Corros. Sci.,* 2010, vol. 52, p. 4046.
8. Kosari, A., Moayed, M.H., Davoodi, A., et al., *Corros. Sci.*, 2014, vol. 78, p. 145.
9. Jamal Abdul Nasser, A., and Anwar Sathiq, M., *Int. J. Eng. Sci. Technol.,* 2010, vol. 2, p. 6420.
10. Singh, A.K. and Quraishi, M.A., *J. Appl. Electrochem.,* 2010, vol. 40, p. 1297.
11. Jacob, K.S. and Parameswaran, G., *Corros. Sci.,* 2010, vol. 52, p. 224.
12. Oguzie, E.E., Wang, S.G., Li, Y., et al., *J. Phys. Chem.*, 2009, vol. 113, p. 8424.
13. De Sousa, F.S. and Spinelli, A., *Corros. Sci.*, 2009, vol. 51, p. 645.
14. Antonijevic, M.M. and Petrovic, M.B., *Int. J. Electrochem. Sci.*, 2008, vol. 3, p. 28.
15. Kokalj, A., Peljhan, S.M., Finsgar, I., et al., *J. Am. Chem. Soc.*, 2010, vol. 132, p. 16664.
16. Abeda, J., Anne, K., Duhme, K., et al., *J. Chem. Soc., Dalton Trans.*, 2012, vol. 41, p. 91.
17. Ita, B.I., *Bull. Chem. Soc. Ethiop.,* 2006, vol. 20, p. 254.
18. James, S.J.P., *J. Comput. Chem.*, 1989, vol. 10, p. 209.
19. Okafor, P.C., Ebenso, E.E., and Ekpe, U.J., *Bull. Chem. Soc. Ethiop.*, 2004, vol. 18, p. 181.
20. Benabdellah, M., Khaled, K.F., and Hammouti, B., *Mater. Chem. Phys.*, 2010, vol. 120, p. 61.
21. Ebenso, E.E., Okafor, P.C., Offiong, O.E., et al., *Bull. Electrochem.,* 2001, vol. 17, p. 259.
22. Solmaz, R., *Corros. Sci.*, 2014, vol. 79, p. 169.
23. Lukovits, I., Kalman, E., and Palinkas, G., *Corrosion*, 1995, vol. 51, p. 201.
24. Moretti, G., Quartarone, G., Tassan, A., et al., *Electrochim. Acta*, 1996, vol. 41, p. 1971.
25. Shukla, S.K. and Quraishi, M.A., *Corros. Sci.*, 2009, vol. 51, p. 1010.
26. Fouda, S., Al-Sarawy, A., Ahmed, F., et al., *Corros. Sci.*, 2009, vol. 51, p. 485.
27. Khadom, A.A., Yaro, A. S., and Kadhum, A.A.H., *J. Chil. Chem. Soc.*, 2010, vol. 55, p. 150.
28. El-Awady, A., Abd-El-Nabey, A., and Aziz, G., *J. Electochem. Soc.*, 1992, vol. 139, p. 2149.
29. Abboud, Y., Abourrich, A., Saffaj, T., et al., *Appl. Surf. Sci.*, 2006, vol. 252, p. 8184.
30. Moretti, G. and Guidi, F., *Corros. Sci.*, 2002, vol. 44, p. 2000.
31. Moretti, G., Guidi, F., and Grion, G., *Corros. Sci.*, 2004, vol. 46, p. 390.
32. Onen, A.I., Nwufo, B.T., Ebenso, E.E., et al., *Int. J. Electrochem. Sci.*, 2010, vol. 5, p. 1570.
33. Musa, A.Y., Kadhum, A.A.H., Mohamad, A.B., et al., *J. Mol. Struct.* 2010, vol. 969, p. 233.
34. Fang, J. and Li, J., *J. Mol. Struct.: THEOCHEM*, 2002, vol. 593, p. 179.
35. Bereket, G., Hur, E., and Oğretir, C., *J. Mol. Struct.: THEOCHEM*, 2002, vol. 578, p. 79.
36. Wazzan, N.A. and Mahgoub, F.M., *Open J. Phys. Chem.*, 2014, vol. 4, p. 8.
37. Nataraja, S.E., Venkatesha, T.V., Tandon, H.C., et al., *Corros. Sci.,* 2011, vol. 53, p. 4112.
38. Ju, H., Kai, Z., and Li, Y., *Corros. Sci.*, 2008, vol. 50, p. 865.
39. Lukovits, I., Kalman, E., and Zucchi, F., *Corrosion,* 2001, vol. 57, p. 3.
40. Parr, R.G. and Pearson, R.G., *J. Am. Chem. Soc.*, 1983, vol. 105, no. 26, p. 7516.